Study on particulate silica networks in natural rubber from the viewpoint of reinforcing effect

Atitaya TOHSAN

1. INTRODUCTION

Natural rubber (NR) has been widely recognized as a useful soft mater, which is both highly elastic and crystallizable under high strains [1-3]. NR is indispensable for manufacturing pneumatic tires of heavy-duty uses *e.g.* those for aircrafts, heavy trucks and rubber bearings in a seismic isolation system [1-4]. Thin NR films, which are directly prepared from NR latex without coagulation, are also very important materials for biomedical and health care fields [1,5,6]. These extensive applications of NR are based on its high elasticity and excellent mechanical strength. The latter is ultimately attributable to its ability of crystallization upon stretching [1-4,7-11]. Therefore, it is necessary to evaluate the strain-induced crystallization (SIC) behavior for development of high performance NR materials.

Up to now, the SIC behavior of NR have been extensively studied [7-26]. A general tendency of the SIC behavior of NR was thus established [16-19]: Upon tensile deformation, polymer chains start to be stretched. Among the polymer chains, short ones are fully-stretched first, and these fully-stretched chains can act as precursors for crystallization like a nucleus of crystallites. Therefore, the NR crystallites are usually observed to grow up in the direction perpendicular to the molecular chain axis [22,23].

Reinforcing fillers, on the other hand, have been known to be of remarkable influence on the SIC of NR because of their strong interfacial interactions with the polymer matrix. Studies on the SIC behavior of carbon black/NR composites have been especially focused due to the importance for heavy-duty uses [21,22,27-30]. Among these studies, there are some common observations: By the inclusion of carbon black, a start of SIC shifted to a lower strain, *i.e.*, the SIC was apparently accelerated. This tendency was, however at least partially explained due to the decrease of volume fraction of NR in the material by the isotropic filler inclusion. In terms of crystallinity, it was commonly observed to linearly increase with an increase of strain similarly with non-filled NR. These phenomena were also detected in commercial silica filled NR-based composites [29] and *in situ* silica filled one [23]. Recently, we prepared novel biphasic structured *in situ* silica filled NR composites by a sol-gel reaction of tetraethoxysilane using *n*-butylamine in NR latex [31]. This preparation procedure is a kind of soft process as the composites were prepared by liquid-state mixing and followed by casting to obtain thin films. In the composites, the *in situ* silica was locally dispersed around rubber particles to result in the specific morphology. Namely, NR particles in the latex worked as templates to form the novel biphasic structure in the composites. The rubber phase in the biphasic structure was of higher purity than that of the composite prepared by conventional mechanical mixing. Thus, unique dynamic mechanical properties were detected in the composites. In order to further clarify the characteristics of the biphasic structured *in situ* silica filled NR composites, the simultaneous synchrotron wide-angle X-ray diffraction (WAXD) and tensile measurements were conducted in this study. Nowadays, *in situ* generated silica in a rubbery matrix moves forward into the nano-technology [32-34]. Therefore, present results will be useful for further developing of rubber-based nano-composites.

2. EXPERIMANTAL

2.1 Materials Sulfur cross-linked and uncross-linked *in situ* silica filled NR composites were used in this study, which were prepared by the soft processing method [31]. The former and the latter are abbreviated as S-NR-Si and NR-Si, respectively. Their *in situ* silica contents were 10 phr. An unfilled sulfur cross-linked NR film (S-NR) was similarly prepared [31] and used as a reference sample. All specimens subjected to the measurements in this study were virgin samples.

Images of transmission electron microscopy (TEM) for S-NR-Si and NR-Si are displayed in Fig. 1 [31]. Dark phases show the generated *in situ* silica. It is worth noting that the *in situ* silica was dispersed around the rubber phases (the bright phases in the photographs) and there was little silica inside the rubber phases. Therefore, the characteristic morphology of *in situ* silica may be a model of a filler network in the rubber matrix. The filler network seems to be fallen into different sizes, which is ascribable to different sizes of NR particles in the latex.

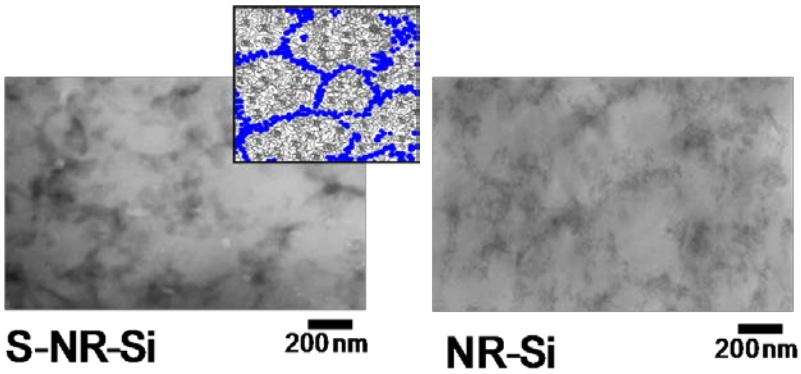

Fig 1. TEM photographs of the *in situ* silica filled NR composites.

2.2 Simultaneous Wide-angle X-ray Diffraction and Tensile Measurements

Simultaneous WAXD and tensile measurements were carried out using a synchrotron radiation system at BL-40XU beam line of SPring-8 in Harima, Japan [35]. A custom-made tensile tester (ISUT-2201, Aiesu Giken Co., Kyoto) was situated on the beam line, and WAXD patterns were recorded during the tensile measurement at room temperature (*ca*. 25 °C). The wavelength of the X-ray was 0.0832 nm and the camera length was 198 mm. Two-dimensional WAXD patterns were recorded using a CCD camera (ORCA II, Hamamatsu Photonics, Co.). Intensity of the incident X-ray was attenuated using a rotating slit equipped on the beam line, and the incident beam was exposed on the sample for 40 ms every 3 s. The intensities of the incident beam and transmitted beam through air were measured using ion chambers. A ring-shaped sample was subjected to the tensile measurement in order to correctly measure the stretching ratio (α) of deformed sample. The stretching speed was 100 mm/min, *i.e*., strain speed was *ca*. 4.98 per min. An absorption correction for thinning of the sample under stretching was carried out using calculated correction coefficients, which were estimated on the basis of absorption coefficients per density [36] and weight fractions of each element in the sample. Here, an affine deformation was assumed for all rubber samples on the basis of their measured Poisson's ratios.

2.3 WAXD Analysis The obtained WAXD images were processed using a software "POLAR" (Stonybrook Technology & Applied Research, Inc.) [15]. Each WAXD pattern of stretched sample was decomposed into three components, *i.e.*, isotropic, oriented amorphous and crystalline components. Three components were azimuthally integrated within the range of ±75° from the equator; the details of this analytical method were described in our previous papers [16,17]. Two structural parameters were estimated at first, of which "crystallinity index" (*CI*) and "oriented amorphous index" (*OAI*) are defined by the following equations.

$$CI = \frac{\sum_{\text{crystal}} 2\pi \int \sin\phi d\phi \int I(s)s^2 \mathrm{d}s}{\sum_{\text{total}} 2\pi \int \sin\phi d\phi \int I(s)s^2 \mathrm{d}s} \quad (1)$$

$$OAI = \frac{\sum_{\text{oriented amorphous}} 2\pi \int \sin\phi d\phi \int I(s)s^2 \mathrm{d}s}{\sum_{\text{total}} 2\pi \int \sin\phi d\phi \int I(s)s^2 \mathrm{d}s} \quad (2)$$

By summation of *CI* and *OAI*, the oriented index (*OI*) can be obtained. In eqs. 1 and 2, $I(s)$ represents the intensity distribution of each peak that is read out from the WAXD pattern, s is the radial coordinate in reciprocal space in nm^{-1} unit ($s = 2(\sin\theta/\lambda)$, where λ is the wavelength and 2θ is the scattering angle), and φ is the angle between the scattering vector of the peak and the fiber direction.

3. RESULTS AND DISCUSSION

3.1 Tensile Characteristics of *In Situ* Silica Filled NR Composites Prepared by the Soft Processing Method

Tensile stress-strain curves up to mechanical rupture points of the *in situ* silica filled NR composites, i.e., S-NR-Si and NR-Si are shown in Fig. 2(a) with that of S-NR. Note that NR-Si was not chemically cross-linked but was physically cross-linked due to aggregation of non-rubber components in NR [25] and hydrogen-bonding between silica and rubber particles. It is clearly seen that the *in situ* silica filled composites, both cross-linked and uncross-linked ones, showed higher stresses than the unfilled sample up to stretching ratio of ca.6. This is basically ascribable to reinforcement effect of the *in situ* silica. The sulfur cross-linking also increased the tensile stress of the *in situ* silica filled biphasic structured composite. For NR-based materials, an effect of SIC on the mechanical properties has to be also taken into account, because the strain-induced crystallites may play a role to increase the stress. Thus, simultaneous time-resolved WAXD and tensile measurements for these samples were carried out *in situ* in this study.

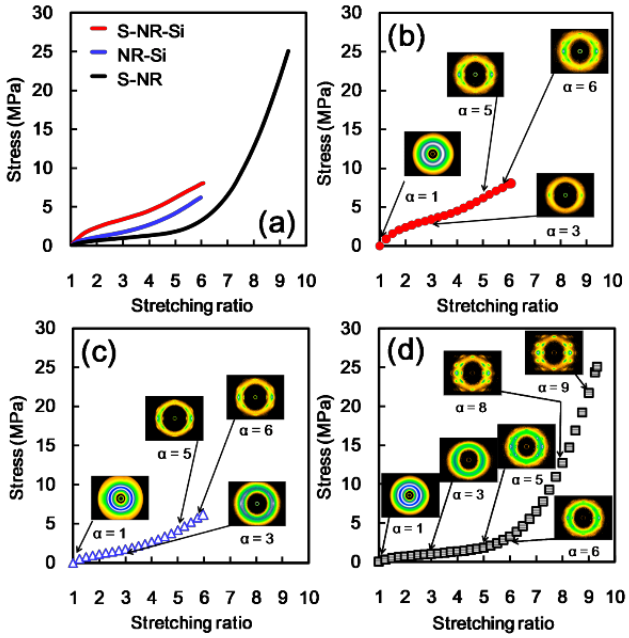

Fig 2. Tensile stress-strain curves of the samples (a), WAXD images at stretching ratio of 1, 3, 5, 6, 8 and 9 showing SIC behaviours of S-NR-Si (b), NR-Si (c) and S-NR (d), respectively.

3.2 SIC of *In Situ* Silica Filled NR Composites Prepared by the Soft Processing Method

WAXD images at α = 1, 3, 5, and 6 of the three samples are displayed in Fig. 2(b) - (d) together with their stress-strain curves. Plotted spots in the curves indicate events of X-ray irradiation in the WAXD measurements. For S-NR, WAXD images at α = 8 and 9 are also displayed in Fig. 2(d). Note that a background scattering by air was removed from their WAXD patterns. Initially, all samples showed only one broad ring at α = 1, *i.e.*, they were totally amorphous before stretching. The SIC started at $1 < \alpha < 3$ in the silica filled samples, while the unfilled sample was not yet crystallized at α = 3 and its SIC was detected at high stretching ratio. Consequently, the remained large content of un-oriented segments under the presence of strain-induced crystallites can be counted as a unique characteristic of polyisoprene chains under tensile deformation. Thus, it is estimated that the three states, i.e., completely amorphous segments, oriented amorphous segments and oriented crystallites are coexisted in the samples. Therefore, the WAXD results were subjected to the analysis to obtain three indexes, *OI*, *OAI* and *CI*, according to the methods in Section 2.5. The results are shown in Fig. 3, respectively.

Since silica particles do not deform upon stretching like rubber, an effective stretching ratio (α_e) was used for the comparison. It is defined by eq. 3 [39],

$$\alpha_e = (\alpha - \gamma)/(1 - \gamma) \qquad (3)$$

where γ is a volume fraction of filler. The density of *in situ* silica used for the calculation was 1.92 g/cm^3 [40-42]. In order to elucidate the effects of *in situ* silica filling and sulfur cross-linking on the SIC of the

composites, strain dependences of *OI*, *OAI* and *CI* are separately shown in Fig. 3(a) - (c) for S-NR-Si and S-NR and in Fig. 3(d) - (f) for S-NR-Si and NR-Si, respectively. All SIC indexes show a tendency to increase with the increasing of strain. However, we observed unique behaviors of SIC, i.e., "a stepwise SIC" for the *in situ* silica filled NR composites, which are distinguishably different with those of reported SIC phenomena as mentioned earlier [7-23,27-30]. Thus, detailed discussions on the stepwise SIC are given in the following sub-sections.

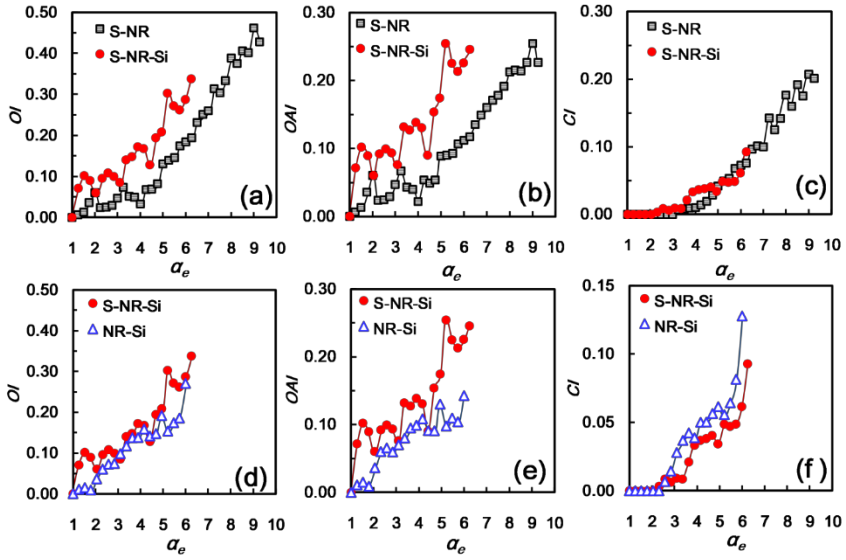

Fig. 3 Variations of *OI* (a) and (d), *OAI* (b) and (e) and *CI* (c) and (f) for S-NR-Si, NR-Si and S-NR, which are plotted against effective stretching ratio. Note that the scale of ordinate in (f) is twice of that in (c). The lines are connected between the data points.

(i) Sulfur Cross-linked *In Situ* Silica Filled NR Composite

As shown in Fig. 3(a), short amorphous (assumed to be Gaussian) network chains of S-NR-Si began to orient immediately upon stretching. However, the *OI* did not increase linearly to the end, *i.e.*, the *OI* repeated a small increase and a small decrease during the upward change. It is important to emphasize that the obtained results are reliable as we obtained a good reproducibility among three fittings for all parameters. Errors among the three fittings for each point were within ± 0.8 % from the each average. Thus, the averages were plotted in the figures. The unique variation of the *OI* was also observed up to ca.5 of α_e in the unfilled S-NR, but the up and down were much smaller and less frequent than those of the composite. The slope of the upward increase was steeper in S-NR-Si than in S-NR. At most of strain region, the *OI* was larger in S-NR-Si than in S-NR.

Strain dependences of *OAI* were very similar with those of *OI* as shown in Fig. 3(b). The *in situ* silica filling in the NR latex was found to promote the orientation of NR chains to the stretching direction upon stretching. However, it is noted that the increase of *OAI* in S-NR-Si showed a few ark-like variations around

1.5, 2.5 and 3.5 of α_e. This observation suggests that the orientation of network chains was significantly restricted by the *in situ* silica in the biphasic structured soft composite. This consideration is supported by strain dependences of *CI* for S-NR-Si. As shown in Fig. 3(c), three steps were detected in the variation of *CI* for S-NR-Si. Note that the region around 5.5 of α_e was judged as one step from the definitive change of orientation fluctuation of strain-induced crystallites (See Section 3.5). This unexpected variation of *CI* is ascribable to the specific morphology of the *in situ* silica filled biphasic structured composite as shown in Fig. 1(a).

By comparing the variation of *OAI* with that of *CI* in S-NR-Si, two tendencies were observed: the *OAI* decreased at each plateau region of *CI*, and the *OAI* increased with the increase of *CI*. These two phenomena are explained as follows: In the cross-linked rubber phase of S-NR-Si, the short amorphous segments began to orient to the stretching direction upon stretching, and to result in the increase of *OAI*. Some of the oriented amorphous segments were crystallized by further stretching to increase the crystallinity. However, it became difficult for the amorphous segments to orient to the stretching direction due to the interruption of chain deformation by the silica layer around the rubber phase. Consequently, the progress of SIC became quite slow to give the plateau region. Once the silica layer was broken upon further stretching, however, the *in situ* silica particles must have been randomly dispersed into the rubbery matrix. Consequently, the rubber chains seemed to be freely extended to result in the acceleration of SIC. As a result, the *OAI* and *CI* increased again.

The speculated SIC behavior of S-NR-Si is schematically illustrated in Fig. 4 with a figure to show the variations of *CI* and *OAI*. The *in situ* silica phases are displayed by connected blue particles around the rubber phases which are expressed by black lines. Black points in the rubber phases are cross-linking sites. Red lines are short rubber chains which connect the cross-linking sites: Before the deformation, the rubber chains are in coil state as shown in Fig. 4(b). When the deformation starts, the short chains orient at first and the *in situ* silica phases also start to be deformed as shown in Fig. 4(c). With the increase of oriented chains upon further stretching, the crystallites are generated in the rubber phases as shown in Fig. 5(d). Under the large deformation, the silica filler network is broken down. Since there are different sizes of rubber phases, the collapse of silica layers occurs successively. Upon further deformation, the silica filler networks are totally broken down and the SIC are promoted similarly with the conventionally filler filled composites as shown in Fig. 4(e). Here, the cartoons are drawn in order to emphasize the variation of one biphasic structure with a silica phase around a rubber phase. In reality, this type of deformation should be taken into account for all rubber phases of different sizes.

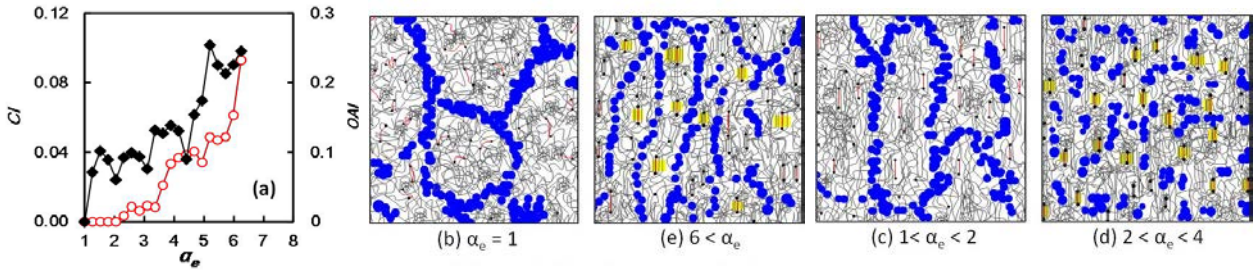

Fig 4. Variations of *OAI* and *CI* plotted against effective stretching ratio for S-NR-Si (a), and its speculated SIC behavior (b) - (e). This deformation occurs in each different sized rubber phase in the sulfur cross-linked *in situ* silica filled NR composite.

Appearance of the stepwise SIC is concluded to be due to the size distribution of the rubber particles in highly ammoniated NR latex as reported [5]. Recently, a dual crystallization behavior was reported in NR-based nanocomposite systems, where nanofiller with a high aspect ratio, *e.g.*, nanoclay [43] and carbon nanotube [44], were used. Differently with these studies, a few steps of SIC shown in Fig. 4 were detected relating with the characteristic feature of the "NR latex template method" combining with the sol-gel reaction of TEOS [31]: The rubber particles in the latex got closer during drying the composite latex, and consequently the densely packed *in situ* generated silica was dispersed around the rubber particles like a boundary layer.

In terms of onset strain of SIC, S-NR-Si showed a crystalline diffraction peak at the lower strain ($\alpha_{e,c}$ = *ca*.2.25) than that of S-NR ($\alpha_{e,c}$ = *ca*.3.5) as shown in Fig. 3(c). The introduction of *in situ* silica apparently accelerated the start of SIC to result in the short induction period of SIC similarly with the composites prepared by a mechanical milling technique [21-23,27-30]. The smaller onset strain of SIC of the reinforced systems is ascribed to two phenomena: The decrease of the volume fraction of rubbery phase at first and the high interfacial interaction between reinforcing fillers and rubbery matrix in the second. The former is a volume effect in general when filled and the latter is dependent on the kind of mixed filler. However, the effective stretching ratio is used for the SIC analyses in this study. Therefore, the small $\alpha_{e,c}$ value of S-NR-Si suggests the presence of strong interfacial interaction between *in situ* silica and the rubber phases.

(ii) Uncross-linked *In Situ* Silica Filled NR Composite

In general, a cross-linking significantly affects the SIC of NR [18,19,24,26]. Since S-NR-Si is a cross-linked sample, the uncross-linked *in situ* silica filled composite (NR-Si) was subjected to the SIC study in order to highlight the effect of *in situ* silica phase on the SIC of NR in the composite. Strain dependences of *OI*, *OAI* and *CI* of NR-Si are shown with those of S-NR-Si in Fig. 3(d) - (f). It is worth noting that network chains oriented only a little upon stretching up to 2.0 of α_e in NR-Si. At the strain region of $2 < \alpha_e < 3$, both *OI* and *OAI* increased and show a small plateau region. From *ca*.3 of α_e, both values increased again upon further stretching and their variations became small around 4.5 of α_e, where a small down was also observed. A shape of variation of *CI* in NR-Si was quite similar with that in S-NR-Si, although the variation in NR-Si began at a lower strain than S-NR-Si and the plateau regions were imperfect.

Comparing the SIC of NR-Si with that of S-NR-Si, a tendency of slower increases of *OI* and *OAI* was observed in the former than in the latter. Due to the absence of cross-linking sites in NR-Si, the orientation of NR chains became slower and its degree was lower in NR-Si than in S-NR-Si. Unexpectedly, however, the SIC of NR-Si was found to give higher *CI* values than that of S-NR-Si as shown in Fig. 3(f). As reported previously, the *in situ* silica located at the surface not in the rubber phase [31]. Therefore, the pure rubber phases inside of silica phases in NR-Si are considered to be more crystallisable upon stretching comparing with S-NR-Si. This phenomenon clearly shows one of the roles of cross-linking sites to prevent the SIC, although the cross-linking sites are also known to accelerate the SIC. This observation may be of use for a material design of high performance rubber products. In terms of onset strain of SIC, the difference between the two composites was minor as shown in Fig. 3(f) in contrast to the observation above, *i.e.*, cross-linked or not shows less influence. The interaction between NR and *in situ* silica may be related with the first orientation of rubber chains.

4. CONCLUSIONS

The time-resolved WAXD measurement during stretching revealed that the SIC of the biphasic structured *in situ* silica filled NR soft composites occurred stepwise, i.e., the degree of crystallinity showed the repetition of increase and standstill cycles. This behaviour was found on the composites prepared from NR latex with *in situ* silica by using the liquid-state mixing and casting methods. The unfilled NR latex vulcanizate prepared by casting also showed the stepwise SIC, although the steps became obscured with the increase of strain. The presence of new biphasic structure in the NR latex vulcanizate brought about the increase of oriented amorphous chains to result in the promotion of SIC, where the generation of small crystallites dominantly occurred stepwise due to the silica phases around the rubber phases. The small crystallites worked as nano-fillers to reinforce NR *via* the oriented amorphous chains. Since the *in situ* silica was not introduced inside the rubber phases but on the surface, the observed characteristic phenomena of the SIC may be of interest in understanding a role of filler network for the reinforcement of rubber. The role has been one of the big questions in rubber science and technology, because the ideal model composite only with filler networks has been difficult to be prepared. For further development of rubber science, a study on the biphasic structured NR composites with different silica contents will be necessary from the viewpoints of silica contents and cyclic deformation, which will be reported in a near future.

REFERENCES

1. Bateman L (1963) The Chemistry and Physics of Rubber-Like Substances. MacLaren & Sons, London.
2. Roberts AD (1988) Natural Rubber Science and Technology. Oxford Science Publications, Oxford
3. Jones KP, Allen PW (1992) Historical Development of the World Rubber Industry. In Sethuraj MR, Mathew NM (ed) Developments in Crop Science, Volume. 23, Natural Rubber: Biology, Cultivation and Technology. Elsevier, Amsterdam, pp 1-22
4. Rodgers B, Waddell W (2005) The science of rubber compounding. In: Mark JE, Erman B, Eirich FR (ed) *The Science and Technology of Rubber*, 3rd ed.; Elsevier Academic Press, Oxford
5. Blackley DC (1997) Polymer Latices Science and Technology Volume 2: Types of Latices, 2nd edn. Chapman & Hall, London
6. Wititsuwanakul D, Wititsuwanakul R, Steinbuchel A (2001). *Biopolymers* Volume 2. Wiley-VCH, Weinheim, Germany
7. Katz JR (1925) Röntgenspektrographische Untersuchungen am gedehnten Kautschuk und ihre mögliche Bedeutung für das Problem der Dehnungseigenschaften dieser Substanz. Naturwiss 19: 410-418
8. Flory PJ (1953) Principles of polymer chemistry. Cornell University. Ithaca, New York
9. Treloar LRG (1975) *The physics of rubber elasticity.* Clarendon Press, Oxford
10. Mitchell GR (1984) A wide-angle X-ray study of the development of molecular orientation in crosslinked natural rubber. Polymer 25:1562-1572
11. Mandelken L (2002) Crystallization of Polymers Volume 1: Equilibrium concepts. 2nd ed. Cambridge University Press. Cambridge
12. Andrews EH (1962) Spherulite morphology in thin films of natural rubber. Proc R Soc A 270:232-241
13. Tsuji M, Kohjiya S (1995) Structural studies on crystalline polymer solids by high-resolution electron

microscopy. Prog Polym Sci 20:259–308

14. Murakami S, Senoo K, Toki S, Kohjiya S (2002) Structural development of natural rubber during uniaxial stretching by *in situ* wide angle X-ray diffraction using a synchrotron radiation. Polymer 43:2117-2120
15. Toki S, Sics I, Ran S, Liu L, Hsiao BS, Murakami S, Senoo K, Kohjiya S (2002) New insights into structural development in natural rubber during uniaxial deformation by *in situ* synchrotron X-ray diffraction. Macromolecules 35:6578-6584
16. Tosaka M, Murakami S, Poompradub S, Kohjiya S, Ikeda Y, Toki S, Sics I, Hsiao BS (2004) Orientation and crystallization of natural rubber network as revealed by WAXD using synchrotron rRadiation. Macromolecules 37:3299-3309
17. Tosaka M, Kohjiya S, Murakami S, Poompradub S, Ikeda Y, Toki S, Scis I, Hsiao BS (2004) Effect of network-chain length on strain-induced crystallization of NR and IR vulcanizates. Rubber Chem Technol 77:711-723
18. Ikeda Y, Yasuda Y, Makino S, Yamamoto S, Tosaka M, Senoo K, Kohjiya S (2007) Strain-induced crystallization of peroxide-crosslinked natural rubber. Polymer 48:1171-1175
19. Ikeda Y, Yasuda Y, Hijikata K, Tosaka M, Kohjiya S (2008) Comparative study on strain-induced crystallization behavior of peroxide cross-linked and sulfur cross-linked natural rubber. Macromolecules 41:5876-5884
20. Che J, Toki S, Valentin JL, Brasero J, Nimpaiboon A, Rong L, Hsiao BS (2012) Chain dynamics and strain-induced crystallization of pre- and postvulcanized natural rubber latex using proton multiple quantum NMR and uniaxial deformation by *in situ* synchrotron X-ray diffraction. Macromolecules 45:6491-6503
21. Poompradub S, Tosaka M, Kohjiya S, Ikeda Y, Toki S, Sics I, Hsiao BS (2005) Mechanism of strain-induced crystallization in filled and unfilled natural rubber vulcanizates. J Appl Phys 97:103529/1-103529/9
22. Ikeda Y, Kato A, Shimanuki J, Kohjiya S, Tosaka M, Poompradub S, Toki S, Hsiao BS (2007) Nano-structural elucidation in carbon black loaded NR vulcanizate by 3D-TEM and *in situ* WAXD measurements. Rubber Chem Technol 80(2):251-264.
23. Ikeda Y, (2005) Green nano-composites prepared from natural rubber and *in situ* silica. Kautsch Gummi Kunstst 58:455-460
24. Ikeda Y, Higashitani N, Hijikata K, Kokubo Y, Morita Y, Shibayama M, Osaka N, Suzuki T, Hitoshi E, Kohjiya S (2009) Vulcanization: new focus on a traditional technology by small-angle neutron scattering. Macromolecules 42:2741-2748
25. Karino T, Ikeda Y, Yasuda Y, Kohjiya S, Shibayama M (2007) Nonuniformity in natural rubber as revealed by small-angle neutron scattering, small-angle X-ray scattering, and atomic force microscopy. Biomacromolecules 8:693-699
26. Suzuki T, Osaka N, Endo H, Shibayama M, Ikeda Y, Asai H, Higashitani N, Kokubo Y, Kohjiya S (2010) Nonuniformity in cross-linked aatural rubber as revealed by contrast-variation small-angle neutron scattering. Macromolecules 43(3):1556-1563
27. Gehman SD, Field JE (1941) X-Ray structure of rubber-carbon Black MixturesRubber Chem Technol 14:85-97
28. Trabelsi S, Albouy PA, Rault J (2003) Effective local deformation in stretched filled rubber. Macromolecules 36(24):9093-9099

29. Chenal JM, Gauthier C, Chazeau L, Guy L, BomalY (2007) Parameters governing strain induced crystallization in filled natural rubber. Polymer 48:6893-6901
30. Dupres S, Long DR, Albouy PA, Sotta A (2009) Local deformation in carbon black-filled polyisoprene rubbers studied by NMR and X-ray diffraction. Macromolecules 42:2634–2644
31. Tohsan A, Phinyocheep P, Kittipoom S, Pattanasiriwisawa W, Ikeda Y (2012) Novel biphasic structured composite prepared by *in situ* silica filling in natural rubber latex. Polym Adv Tech 23:1335–1342
32. Mark JE, Pan SJ (1982) Reinforcement of poly(dimethylsiloxane) networks by *in situ* precipitation of silica: a new method for preparation of filled elastomers. Makromol Che Rapid Commun 3:681–685
33. Brinker CJ, Scherer GW (1990) Sol-gel science: the physics and chemistry of sol-gel processing, Academic Press, New York
34. Kohjiya S, Ikeda Y (2000) Reinforcement of general-purpose grade rubbers by silica generated *in situ*. Rubber Chem Technol 73:534–550
35. http://www.spring8.or.jp/en/
36. Hahn T (1983) International Tables for Crystallography Vol. A, D. Reidel Pub. Co, Holland
37. Scherrer P (1918) Estimation of the size and internal structure of colloidal particles by means of Röntgen rays. Gottinger Nachrichten 2:96-100
38. Klug HP, Alexander LE (1974) X-ray Diffraction Procedures for Polycrystalline and Amorphous Materials, 2nd ed. Wiley-Interscience, New York
39. Bokobza L (2001) Reinforcement of elastomeric networks by fillers. Macromol Symp 169: 243-260
40. Ikeda Y, Kato A, Shimanuki J, Kohjiya S (2004) Nano-structural observation of *in situ* silica in natural rubber matrix by three dimensional transmission electron microscopy. Macromol Rapid Commun 25:1186-1190
41. Kohjiya S, Kato A, Shimanuki J, Hasegawa T, Ikeda Y (2005) Three-dimensional nano-structure of *in situ* silica in natural rubber as revealed by 3D-TEM/electron tomography. Polymer 46:4440-4446
42. Kohjiya S, Kato A, Ikeda Y (2008) Visualization of nanostructure of soft matter by 3D-TEM:Nanoparticles in a natural rubber matrix. Prog Polym Sci 33:979-997
43. Gonzlez JC, Retso H, Verdejo R, Toki S, Hsiao BS, Emmanuel P, Miguel AL (2008) Effect of nanoclay on natural rubber microstructure. Macromolecules 41: 6763–6772
44. Weng G, Huang G, Qu L, Nie Y, Wu J (2010) Large-scale orientation in a vulcanized stretched natural rubber network: proved by *in situ* synchrotron X-ray diffraction characterization. J Phys Chem B 114:7179-7188
45. Nyburg SC, (1954) A statistical structure for crystalline rubber. Acta Crystallogr 7: 385-392
46. Huneau B (2011) Strain-induced crystallization of natural rubber: A review of X-ray diffraction investigations. Rubber Chem Technol 84: 425–452
47. Che J, Burger C, Toki S, Rong L, Hsiao BS , Amnuaypornsri S, Sakdapipanich J (2013) Crystal and Crystallites Structure of Natural Rubber and Synthetic cis-1,4-Polyisoprene by a New Two Dimensional Wide Angle X-ray Diffraction Simulation Method. I. Strain-Induced Crystallization. Macromolecules 46: 4520–4528
48. Potts JR, Shankar O, Du L, Ruoff RS (2012) Processing–morphology–property relationships and composite theory analysis of reduced graphene oxide/natural rubber nanocomposites. Macromolecules 45: 6045−6055